

Greybody Factor for massive scalar field in charged black hole

Suppawit Polkong

Department of Physics, Faculty of Science, Mahidol University, 272 Rama VI Rd.,
Ratchathewi, Bangkok, 10400, Thailand

Pitayuth Wongjun

The Institute for Fundamental Study (IF), Naresuan University, 99 Moo 9, Tah Poe, Mueang
Phitsanulok, Phitsanulok, 65000, Thailand

Ratchaphat Nakarachinda

The Institute for Fundamental Study (IF), Naresuan University, 99 Moo 9, Tah Poe, Mueang
Phitsanulok, Phitsanulok, 65000, Thailand

Department of Mathematics and Computer Science, Faculty of Science, Chulalongkorn
University, 254 Phaya Thai Rd., Pathum Wan, Bangkok, 10330, Thailand

E-mail: suppawitpolkong@gmail.com

Abstract.

The spectrum of Hawking radiation from black holes can be partially observed due to the spacetime curvature of the black hole behaving like a potential barrier. This spectrum can be described by arranging the Klein-Gordon equation on curved spacetime into the Regge-Wheeler equation. The transmission probabilities of Hawking radiation from this incident are called the greybody factor. In this work, the greybody factor of a massive scalar field in the Reissner-Nordström black hole is investigated using the Wentzel-Kramers-Brillouin (WKB) approximation and rigorous bound methods. As a result, we found that transmission probability and behavior of potential are directly related in such a way that the higher the potential the lower the greybody factor. Both methods achieve a similar conclusion, which states that the greybody factor and mass of the scalar field have an inverse relationship. This can be interpreted in a similar way in quantum mechanics, namely the scalar field with the higher mass will encounter a stronger interaction from the potential and then it is more difficult to penetrate through the potential barrier.

1. Introduction

General Relativity (GR) provides the possibility of the existence of a mysterious object known as a black hole. With observational data [1, 2], it suggests that black holes can exist in the real world. Moreover, the observational data provide a way to constrain black hole parameters characterized by any deviation from GR [3, 4, 5, 6, 7]. These provide the reason why the study of black holes receives much attention nowadays.

One of the most important characteristic behaviors is that black holes behave as thermal systems. Particularly, black holes carry entropy and can emit a type of radiation called Hawking

radiation [8, 9]. As a result, at the event horizon, the spectrum of the radiations from black holes is the same as that of the black-body spectrum. By taking the curvature of spacetime into account, the Hawking radiation is modified while propagating to spatial infinity. The greybody factor is defined as the ratio of the radiation at spatial infinity to that from the emitter by black holes. In fact, in terms of quantum mechanics, the greybody factor corresponds to the transmission amplitude of the wave where the curvature of the spacetime due to the black hole acts as the potential barrier.

The greybody factors from various kinds of spacetime geometry have been intensively investigated by various methods. One of the proper choices intensively investigated in literature is that of using WKB approximation [10, 11, 12, 13, 14, 15, 16, 17]. It provides a good approximation for a simple form of spacetime geometries, and requires the higher potential, or in other words, requires the high multipole. The other useful choice that allows us to study the behavior of the greybody factor analytically is to investigate the greybody factor is to consider the bound of the greybody factor instead of the exact one known as rigorous bound method [18, 19, 20, 21, 22, 23, 24, 25]. In this paper, we are interested in investigating the greybody factor as the massive scalar field emitted from the charged black hole by using WKB approximation and rigorous bound methods. The results from both methods are compared in order to find possible and useful ways to obtain, and analyze the behavior of the greybody factor.

This paper is organized as follows. In Sec. 2, the Schrödinger-like equation for the radial part of the considered massive scalar field is derived. The various methods of solving the aforementioned equation for the greybody factor are discussed and the results are reported in Sec. 3 for the WKB approximation and Sec. 4 for the rigorous bound methods. Sec. 5 is devoted to conclusions.

2. Regge-Wheeler equation

Let us consider a massive scalar field $\Phi(x^\mu)$ on the static and spherically symmetric spacetime which is simply described by the form of the line element:

$$ds^2 = -f(R)dt^2 + \frac{1}{f(R)}dR^2 + R^2(d\theta^2 + \sin^2\theta d\phi^2), \quad (1)$$

where $f(R)$ is the horizon function. Note that this form of metric is obtained from the specific condition on the components of the energy-momentum tensor $T^t_t = T^R_R$. The dynamics of the field obey the Klein-Gordon equation:

$$\frac{1}{\sqrt{-g}}\partial_\mu(g^{\mu\nu}\sqrt{-g}\partial_\nu\Phi) - M_\Phi^2\Phi = 0, \quad (2)$$

where M_Φ is the mass of the field. Employing the separation of variable method and imposing the form of the field given by

$$\Phi(t, R, \theta, \phi) = T(t)\frac{\psi(R)}{R}\Theta(\theta, \phi) \quad (3)$$

Plugging it into Eq. (2), one finds that the form of the temporal and angular parts satisfying their own equations are, respectively, expressed as

$$T(t) = e^{i\Omega t}, \quad \Theta(\theta, \phi) = Y_{lm}(\theta, \phi), \quad (4)$$

where Ω is a constant and $Y_{lm}(\theta, \phi)$ is the spherical harmonics with a non-negative integer l and integer m where $l \geq |m|$. As a result, the leftover is the radial part which can be written in the Schrödinger-like equation as

$$\frac{d^2\psi(R)}{dR^{*2}} + [\Omega^2 - V(R)]\psi(R) = 0, \quad (5)$$

with the potential $V(R)$ given by

$$V(R) = f(R) \left[\frac{l(l+1)}{R^2} + \frac{f'(R)}{R} + M_\Phi^2 \right]. \quad (6)$$

Here, the tortoise coordinate R^* is introduced as $R^* = \int |f(R)|^{-1} dR$. In this coordinate, the black hole's outer horizon $R_h = GM + \sqrt{G^2 M^2 - GQ^2}$ satisfying $f(R_h) = 0$ is mapped to negative infinity $R^* \rightarrow -\infty$. The prime denotes the derivative with respect to the radial coordinate. Eq. (5) also known as the Regge-Wheeler equation describes the dynamics of the field ψ through the potential barrier due to spacetime curvature with frequency (or energy) ω .

In this study, we are interested in the charged black hole described by the horizon function:

$$f(R) = 1 - \frac{2GM}{R} + \frac{GQ^2}{R^2}, \quad (7)$$

where M, Q and G are the mass of the black hole, electric charge, and Newton's gravitational constant, respectively. For convenience, let us work with the dimensionless variables by rescaling the variable with M and G as follows:

$$r = \frac{R}{GM}, \quad q = \frac{Q}{M\sqrt{G}}. \quad (8)$$

The variables in the perturbation equation can be expressed in the dimensionless version as

$$\omega = GM\Omega, \quad m_\Phi = GMM_\Phi, \quad v(r) = G^2 M^2 V(R). \quad (9)$$

The profiles of the potential for various values of the parameters are illustrated in Fig. 1. The asymptotic values of the potential at the black hole's outer horizon and spatial infinity can be, respectively, determined as

$$v(r^* \rightarrow -\infty) = v\left(r \rightarrow r_h = 1 + \sqrt{1 - q^2}\right) = 0, \quad (10)$$

$$v(r^* \rightarrow \infty) = v(r \rightarrow \infty) = m_\Phi^2. \quad (11)$$

It is also observed that the potential can have local maximum and minimum points denoted as v_{\max} and v_{\min} , respectively. The radial distance associated with v_{\max} is always smaller than that associated with v_{\min} , i.e., $r_{v_{\max}} < r_{v_{\min}}$. Note also that the value of the potential at the local minimum is always less than the value at asymptotic infinity, $v_{\min} < m_\Phi^2$. However, the maximum value v_{\max} can be all less than, equal to, and greater than m_Φ^2 .

For varying the electric charge (see the top panels of Fig. 1), when the charge increases, the extremum points of the potential shift to smaller radii and have higher values, and vice versa. In addition, at the chargeless limit (corresponding to the Schwarzschild black hole), the trend of the potential does not change.

As seen in the bottom panels of Fig. 1, the perturbed field's mass is varied. It is interestingly found that the local maximum and minimum points of the potential can coincide if m_Φ is sufficiently large. From the numerical analysis, by setting $q = 0.1$, the extremum points merges when $m_\Phi|_{v_{\max}=v_{\min}} \approx 0.250$ at $r \approx 3.993$ for $l = 0$, and $m_\Phi|_{v_{\max}=v_{\min}} \approx 0.466$ at $r \approx 5.263$ for $l = 1$. Therefore, if the field's mass is larger than the critical value, the potential for given q and l is a monotonically increasing function of r , and maximizes as $v(r \rightarrow \infty) = m_\Phi^2$. In addition, in the small-mass regime, one can split the field mass into two sub-regimes corresponding to $v_{\max} > m_\Phi^2$ for smaller mass, $v_{\max} < m_\Phi^2$ for larger mass. For example, these two sub-regimes are separated by the critical mass (given $q = 1$) as $m_\Phi \approx 0.193$ for $l = 0$ and $m_\Phi \approx 0.398$ for $l = 1$.

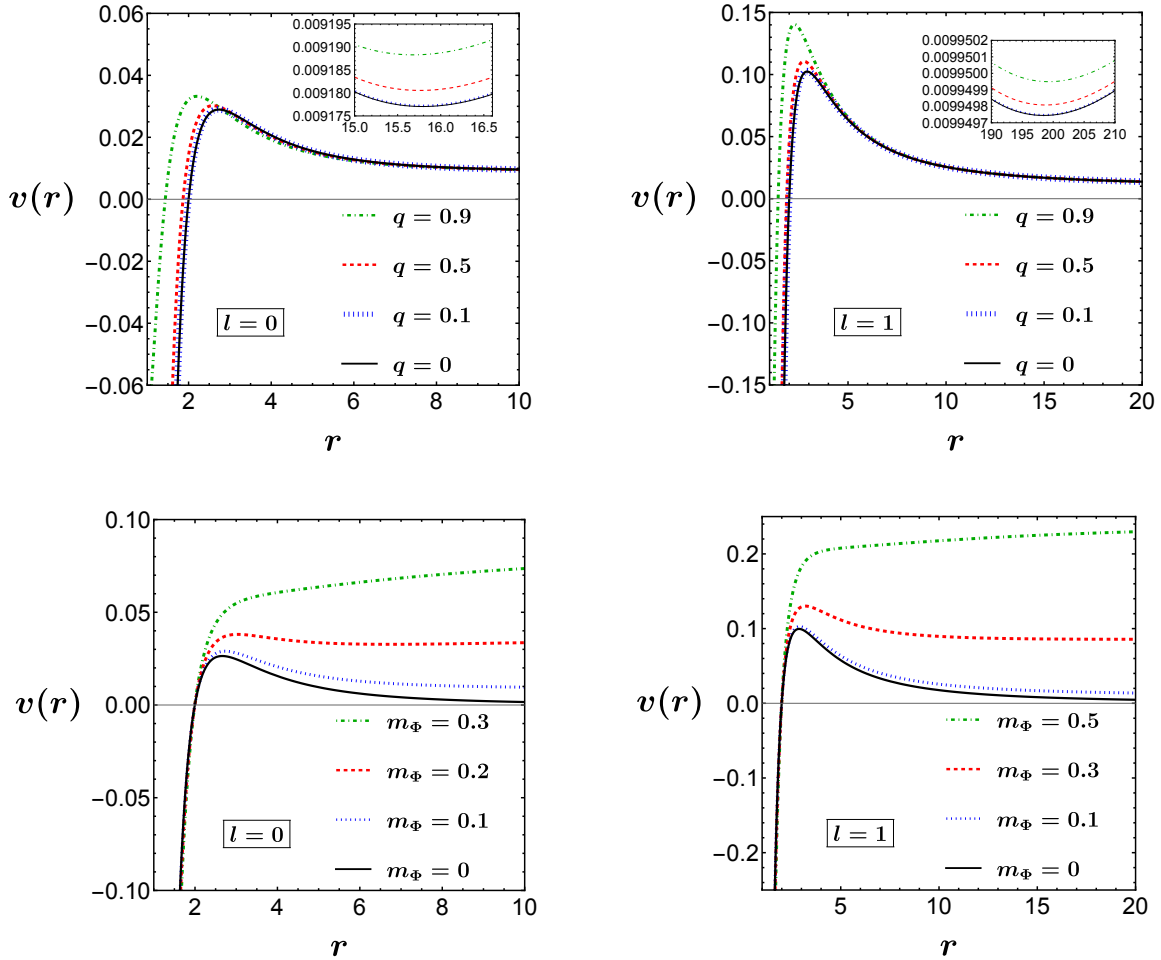


Figure 1: Behaviors of potential for varying charge q with $m_\Phi = 0.1$ (top), and those for varying field's mass m_Φ with $q = 0.1$ (bottom).

These are the significant differences between the massless and massive (with sufficiently large m_Φ) scenarios of the perturbed field. Another remark is that the potential is always non-negative for any radius outside the black hole's horizon.

So far, one can see that the curvature of the spacetime plays a role in the potential barrier. The radial part of the wave function corresponding to the perturbed scalar field penetrates through such a potential similar to the particle in the potential well in quantum mechanics. In the next sections, we aim to determine the greybody factor which is equivalent to the transmission probability using the WKB approximation and rigorous bound methods.

3. Greybody factors from WKB approximation method

The key idea of the WKB approximation is the use of series expansion to obtain the solution. The coefficients of series expansion can be obtained by matching the solutions at the boundaries in which the frequency of the particle is equal to the potential. Therefore, in order to perform the calculation properly, one can separate the consideration into three cases; low-frequency, intermediate-frequency, and high-frequency regimes of the particle. For the high-frequency case, most of the particles can penetrate through the potential so that it is a trivial case. We will omit the consideration for this case in this article. It is convenient to redefine the Schrödinger-like

equation in Eq. 5 as follows:

$$\left(\frac{d^2}{dr^{*2}} + Q \right) \psi = 0, \quad (12)$$

where $Q = \omega^2 - v(r)$.

3.1. Intermediate-frequency approximation ($\omega^2 \approx v_{max}$)

For the intermediate frequency approximation, one cannot apply the WKB method directly since the solutions cannot be matched at the boundary. In order to overcome such obstruction, one can expand the potential around the maximum point for the solution evaluated in the region $\omega^2 < v_{max}$ [10, 11, 12, 13]. By using this idea and following the procedure found in [12], the greybody factor can be obtained as follows:

$$T = \frac{1}{1 + \exp[2S(\omega)]}, \quad (13)$$

where the function S is written as

$$S(\omega) = \pi k^{\frac{1}{2}} \left[\frac{1}{2} z_0^2 + \left(\frac{15}{64} b_3^2 - \frac{3}{16} b_4 \right) z_0^4 + \left(\frac{1155}{2048} b_3^4 - \frac{315}{256} b_3^2 b_4 + \frac{35}{128} b_4^2 + \frac{35}{64} b_3 b_5 - \frac{5}{32} b_6 \right) z_0^6 \right] \\ + \frac{\pi}{k^{\frac{1}{2}}} \left[\left(\frac{3}{16} b_4 - \frac{7}{64} b_3^2 \right) - \left(\frac{1365}{2048} b_3^4 - \frac{525}{256} b_3^2 b_4 + \frac{85}{128} b_4^2 + \frac{95}{64} b_3 b_5 - \frac{25}{32} b_6 \right) z_0^2 \right] + \mathcal{O}(\omega). \quad (14)$$

Note that shot-hand variables evaluated at the maximum of the potential can be defined as follows

$$z_0^2 = -\frac{Q_{max}}{k}, \quad k = \frac{1}{2} \frac{d^2 Q}{dx^2}, \quad b_n = \frac{1}{n!k} \frac{d^n Q}{dx^n}, \quad (15)$$

where $\mathcal{O}(\omega)$ denotes the higher order terms.

3.2. Low-frequency approximation ($\omega^2 \ll v_{max}$)

In this case, the classical turning points where $\omega^2 = v$ will be much farther apart compared to the previous case and denoted by r_1 (smaller radius) and r_2 (larger radius). By using the low-frequency approximation, the greybody factor can be expressed as [12]

$$T = \exp \left(-2 \int_{r_1}^{r_2} \sqrt{v - \omega^2} dr^* \right) \quad (16)$$

From this expression, one can see that the turning points can be obtained by specifying the value of ω . Therefore, we need to evaluate the greybody factor point by point. Moreover, since the potential is complicated and cannot be analytically performed the integration, we will use the numerical method for this case.

3.3. Results

By comparing the greybody factor to the shape of the potential, it is found that the results from the WKB approximation are in the same trend as found in quantum mechanics. Specifically, the higher the potential the lower the greybody factor. This can be illustrated in Fig 2. Note that results from the WKB approximation provide a good estimation for the high value of l and lower value of m_Φ . This is due to the fact that at the lower value of l or higher value of m_Φ , the turning points of the potential are far from together. Therefore, the expansion of the potential around the maximum may not be sufficiently valid. This is the reason why we choose $l = 1$ for the plots in Fig. 2 even though the greybody factor from this mode is much lower than one for the $l = 0$ mode. Note that the results of low-frequency approximation are in agreement with one from intermediate-frequency approximation as shown in the left panel of Fig. 2.

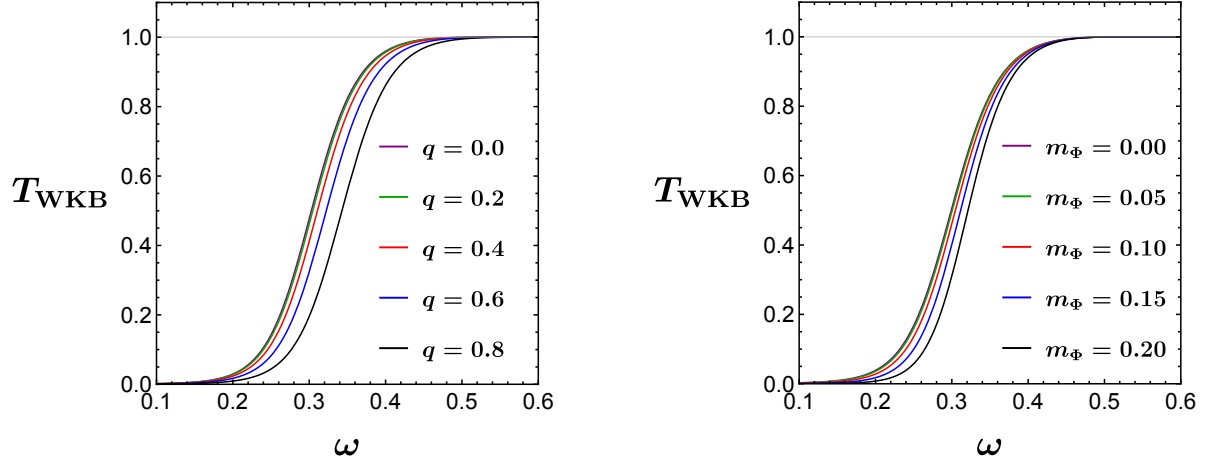


Figure 2: Greybody factor from WKB approximation for $l = 1$. the left panel the parameter q is varied with $m_\Phi = 0.1$ while the right panel the parameter m is varied with $q = 0.2$. dots in the left panel represent the results from low-frequency approximation.

4. Greybody factors from rigorous bound method

One of the other treatments in determining the greybody factor is the so-called rigorous bound method [19, 20]. This method provides the lower bound of the greybody factor. The advantage is the bound can be obtained in analytic form, unlike the results from the WKB method discussed in the previous section. Based on Refs. [19, 20], the lower bound of the greybody factor is given by

$$T \geq \text{sech}^2 \left(\int_{-\infty}^{\infty} \vartheta \, dr^* \right), \quad (17)$$

where

$$\vartheta = \frac{1}{2h(r^*)} \sqrt{h'(r^*)^2 + [\omega^2 - v(r) - h(r^*)^2]^2}, \quad (18)$$

for some positive function $h(r^*)$ satisfying

$$h(\pm\infty) = \sqrt{\omega^2 - v(\pm\infty)}. \quad (19)$$

In this study, we proposed two possible forms of the function $h(r^*)$ in investigating the bound on the greybody factor.

4.1. $h = \sqrt{\omega^2 - v}$

The bound of the greybody factor in Eq. (17) can be written as

$$T \geq T_{\text{bound}} = \text{sech}^2 \left(\frac{1}{2} \int_{-\infty}^{\infty} \frac{|h'|}{h} \, dr^* \right), \quad (20)$$

where the prime denotes the derivative with respect to the tortoise coordinate r^* . Let us start with the large-mass regime so that the potential is monotonically growing in r^* . It implies that $v' > 0$. One then knows that the derivative of the function h for this regime is always negative since

$$h' = -\frac{v'}{2h}. \quad (21)$$

The bound of the greybody factor Eq. (20) can be computed as

$$T_{\text{bound, (large } m_\Phi)} = \text{sech}^2 \left(- \int_{-\infty}^{\infty} \frac{h'}{2h} dr^* \right) = \frac{4\omega \sqrt{\omega^2 - m_\Phi^2}}{\left(\omega + \sqrt{\omega^2 - m_\Phi^2} \right)^2}. \quad (22)$$

The property: $\text{sech}[\ln(x)] = 2x/(1+x^2)$ is also used in the above calculation. According to the above result, this bound exists for the frequency satisfies $\omega \geq m_\Phi$. It is surprising that the bound in such a regime depends only on the perturbed field's mass.

For the small-mass regime, the behaviors of the function h can be split into three ranges of r^* as follows: $-\infty < r^* < r_{v_{\max}}$, $r_{v_{\max}} < r^* < r_{v_{\min}}$, and $r_{v_{\min}} < r^* < \infty$. The bound in Eq. (20) for this regime can be computed as

$$\begin{aligned} T_{\text{bound, (small } m_\Phi)} &= \text{sech}^2 \left(-\frac{1}{2} \int_{-\infty}^{v_{\max}} \frac{h'}{h} dr^* + \frac{1}{2} \int_{v_{\max}}^{v_{\min}} \frac{h'}{h} dr^* - \frac{1}{2} \int_{v_{\min}}^{\infty} \frac{h'}{h} dr^* \right) \\ &= \frac{4\omega \sqrt{\omega^2 - m_\Phi^2} (\omega^2 - v_{\max}) (\omega^2 - v_{\min})}{\left[(\omega^2 - v_{\max}) \sqrt{\omega^2 - m_\Phi^2} + \omega (\omega^2 - v_{\min}) \right]^2}. \end{aligned} \quad (23)$$

It is easily checked that the bound in Eq. (22) can be recovered by taking $v_{\max} = v_{\min}$ in Eq. (23). When $v_{\max} > m_\Phi^2$, the above expression seems to be negative in the range $\sqrt{v_{\min}} < \omega < \sqrt{v_{\max}}$. However, the condition $\omega < \sqrt{v_{\max}}$ makes the function $h = \sqrt{\omega^2 - v}$ not well-defined. The bound of the greybody factor in Eq. (23) is, therefore, valid only in the range $\omega > \sqrt{v_{\max}} (> m_\Phi)$. On the other hand, when $v_{\max} < m_\Phi^2$, the the bound exists in the same region of ω for $T_{\text{bound, (large } m_\Phi)}$, i.e., $\omega \geq m_\Phi$. It is worthwhile to note that the lower bound of the greybody factor T_{bound} depends only on v_{\max} and v_{\min} , not explicitly on the shape of the potential. Hence, it might be difficult to analyze the profile of the bound.

4.2. $h = \sqrt{\omega^2 - fm_\Phi^2}$

The bound of the greybody factor in Eq. (17) for this choice of the function h can be expressed as follows:

$$\begin{aligned} T &\geq \text{sech}^2 \left(\frac{1}{2} \int_{-\infty}^{\infty} \frac{1}{h} \sqrt{h'^2 + (\omega^2 - v - h^2)^2} dr^* \right) \\ &\geq \text{sech}^2 \left(\frac{1}{2} \int_{-\infty}^{\infty} \frac{1}{h} \sqrt{[h' + (\omega^2 - v - h^2)]^2} dr^* \right) \\ &\geq \text{sech}^2 \left(\frac{1}{2} \int_{-\infty}^{\infty} \frac{1}{h} (|h'| + |\omega^2 - v - h^2|) dr^* \right) \\ &= \text{sech}^2 \left[\frac{\ln(h)}{2} \Big|_{-\infty}^{\infty} + \int_{-\infty}^{\infty} \frac{fm_\Phi^2 - v}{2h} dr^* \right] \equiv T_{\text{bound}}, \end{aligned} \quad (24)$$

To obtain the above result, we have used the fact that $h'(\omega^2 - v - h^2) > 0$ in the second line and the triangle inequality: $|x + y| \leq |x| + |y|$ in the third line. After integrating the argument of the hyperbolic secant function in the last line of Eq. (24), the lower bound of the greybody factor can written as

$$T_{\text{bound}} = \text{sech}^2[X], \quad (25)$$

where

$$\begin{aligned}
X = & \frac{1}{4} \ln \left(1 - \frac{m_\Phi^2}{\omega^2} \right) + \frac{m_\Phi q (\omega^2 - m_\Phi^2) + y \sqrt{m_\Phi^2 - \omega^2} \ln \left(\frac{q \sqrt{m_\Phi^2 - \omega^2} - m_\Phi}{q \sqrt{m_\Phi^2 - \omega^2} + m_\Phi} \right)}{2m_\Phi^3 q^3 \sqrt{\omega^2 - m_\Phi^2}} \\
& + \frac{m_\Phi q \omega (q^2 + r_h)(q^2 - 2r_h) - 2y r_h^2 \sqrt{q^2 - 2r_h} \tanh^{-1} \left(\frac{\omega \sqrt{q^2 - 2r_h} - r_h \sqrt{m_\Phi^2 - \omega^2}}{m_\Phi q} \right)}{2m_\Phi^3 q^3 r_h^3}, \quad (26)
\end{aligned}$$

with $y = q^2[(1+l+l^2)m_\Phi^2 - \omega^2] - m_\Phi^2$. Moreover, the integrands X in the Schwarzschild limit ($q \rightarrow 0$) and the massless limit ($m_\Phi \rightarrow 0$) can be, respectively, expressed as

$$\lim_{q \rightarrow 0} X = \frac{1}{4} \ln \left(1 - \frac{m_\Phi^2}{\omega^2} \right) + \frac{\omega^2 \left(\omega - \sqrt{\omega^2 - m_\Phi^2} \right)}{3m_\Phi^4} + \frac{\left(\frac{2}{3} + l + l^2 \right) \sqrt{\omega^2 - m_\Phi^2} - (1 + l + l^2)}{2m_\Phi^2}, \quad (27)$$

$$\lim_{m_\Phi \rightarrow 0} X = \frac{1}{6r_h^3 \omega} \left[\frac{q^2}{2} + 3 \left(\frac{1}{2} + l + l^2 \right) (q^2 - 2r_h) \right]. \quad (28)$$

Obviously, the bound T_{bound} can be explicitly written in terms of the parameters q , m_Φ , and l . It is noticed that the lower bound in Eq. (24) should be lower than those in Eqs. (22) and (23) since the inequality properties have been applied for the sake of integrability. The behaviors of the bounds of the greybody factor associated with both forms of the function h are shown in Fig. 3. As illustrated by this figure, the bound associated with $h = \sqrt{\omega^2 - v}$ is stronger than that associated with $h = \sqrt{\omega^2 - fm_\Phi^2}$ when ω is sufficiently high. On the other hand, in the range of low ω , only the bound associated with $h = \sqrt{\omega^2 - fm_\Phi^2}$ can exist. Hence, they appropriately represent the bound of the greybody factor for different ranges of frequency.

To check the validity of the rigorous bound method, let us compare the bounds with the results approximated by the WKB approximation method in Figs. 4 and 5. It is seen that the bound for given the proposed form of the function h seems to be the proper bound of the greybody factor. Therefore, the rigorous bound method is useful to deal with the problem analytically.

5. Conclusion

In this study, we investigate the greybody factors associated with the massive scalar field on the charged black hole spacetime. It was shown that the dynamics of (the radial part of) the perturbed field can be described by the Regger-Wheeler equation (5) which is taken in the Schrödinger-like form with the effective potential expressed in Eq. (6). One then can interpret that the spacetime curvature acts as a barrier where the wave of the perturbed field penetrates through it. As a general feature of the potential, it gets higher when either q and m_Φ increases. Interestingly, the potential can be the monotonically increasing function in r for the massive scenario with sufficiently large m_Φ . Unlike the massless scenario, it behaves only as a barrier-like form.

The greybody factor for the corresponding wave function was determined using the WKB approximation and rigorous bound methods. With the former method, the results shown in Fig. 2 are reliable because they are in the same trend as the quantum particle does. The greybody factor gets lower as either q or m_Φ increases (causes the higher potential). Therefore, this method provides a good approximation. According to this result, it is possible to conclude

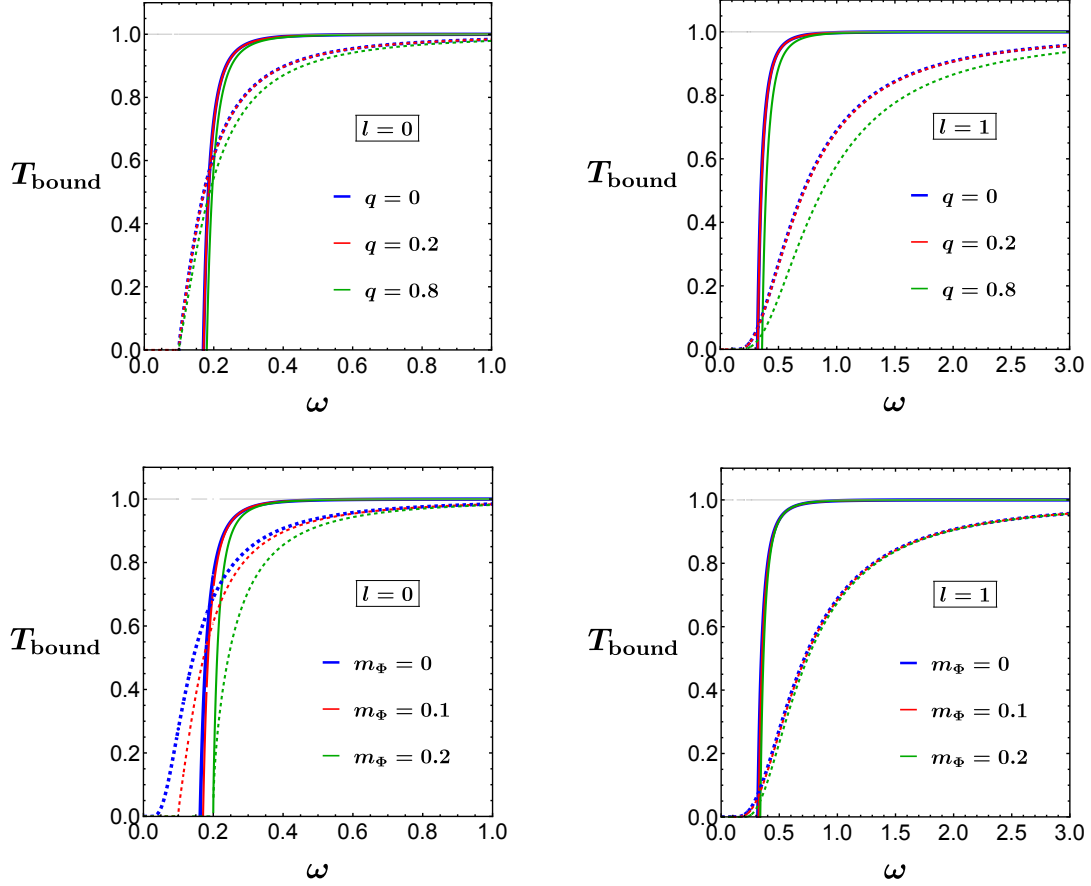


Figure 3: Lower bounds of greybody factor associated with $h = \sqrt{\omega^2 - v}$ represented as solid lines and $h = \sqrt{\omega^2 - fm_\Phi^2}$ represented as dashed lines. The top panels are the plots for various values of q with fixing $m_\Phi = 0.1$ while the bottom are those for various values of m_Φ with fixing $q = 0.2$.

that the perturbed field with higher mass will encounter a stronger interaction due to spacetime curvature and then it is more difficult to penetrate through the potential barrier.

For the latter method, we found that the function $h = \sqrt{\omega^2 - fm_\Phi^2}$ is appropriate to provide the lower bound of the greybody factor in the low-frequency regime while $h = \sqrt{\omega^2 - v}$ yields a stronger bound in the intermediate-frequency regime. As compared these bounds to the results from the WKB approximation method, we have investigated that the results from the rigorous bound method are the proper bounds of the greybody factor.

It is important to remark that, in the large-mass regime as well as the $l = 0$ case, the WKB seems to be inapplicable because the potential is not in a barrier-like form (see Ref. [16] for further discussion). However, the rigorous bound method can deal with this situation. One of the other advantages of the rigorous bound method is that the result (of the bound) is in analytic expression, unlike the numerical result in the WKB approximation method. Therefore, it might be a more powerful tool for studying the physical implications based on the black hole perturbation theory.

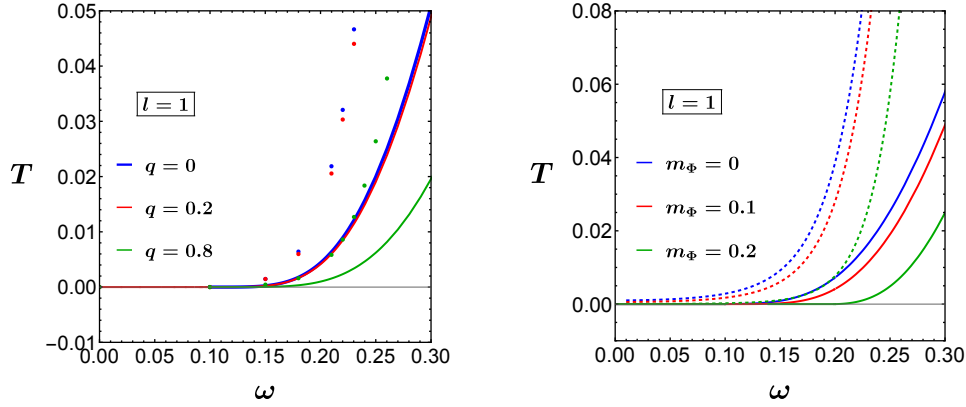


Figure 4: Comparison between the bounds of greybody factor associated with $h = \sqrt{\omega^2 - fm_\Phi^2}$ (for low-frequency regime) represented as solid lines and greybody factor obtained from WKB approximation method represented as dotted or dashed lines for $l = 1$. The parameters q and m_Φ are set as the same as those in Fig. 3.

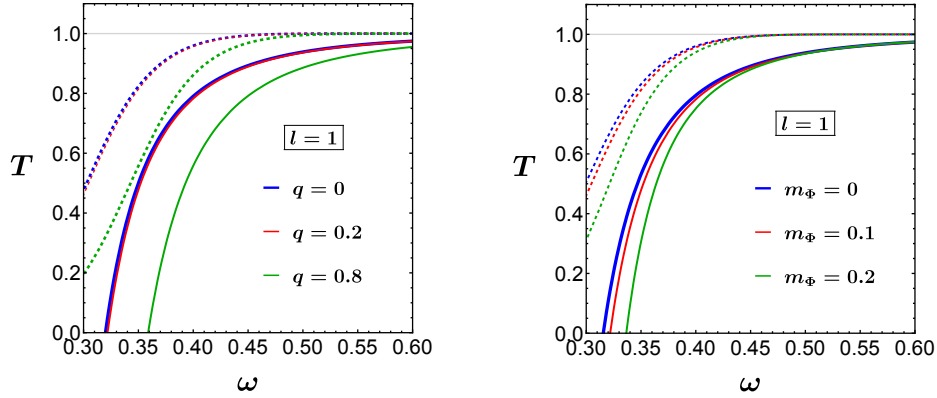


Figure 5: Comparison between the bounds of greybody factor associated with $h = \sqrt{\omega^2 - v}$ (for intermediate-frequency regime) represented as solid lines and greybody factor obtained from WKB approximation method represented as dashed lines for $l = 1$. The parameters q and m_Φ are set as the same as those in Fig. 3.

Acknowledgement

We are grateful to Alejandro Saiz Rivera for providing valuable insight and commentary on this work. This research has received funding support from the NSRF via the Program Management Unit for Human Resources & Institutional Development, Research and Innovation [grant number B39G670016]. SP also acknowledges the support from Sri Trang Thong (STT) scholarship, Faculty of Science, Mahidol University.

- [1] K. Akiyama *et al.* [Event Horizon Telescope], “First M87 Event Horizon Telescope Results. I. The Shadow of the Supermassive Black Hole,” *Astrophys. J.* **875** (2019) no.1, L1 doi:10.3847/2041-8213/ab0ec7 [arXiv:1906.11238 [astro-ph.GA]].
- [2] B. P. Abbott *et al.* [LIGO Scientific and Virgo], “Tests of general relativity with GW150914,” *Phys. Rev. Lett.* **116** (2016) no.22, 221101 [erratum: *Phys. Rev. Lett.* **121** (2018) no.12, 129902] doi:10.1103/PhysRevLett.116.221101 [arXiv:1602.03841 [gr-qc]].
- [3] D. Garofalo, “Spin of the M87 black hole,” *Annalen Phys.* **532** (2020) no.4, 1900480 doi:10.1002/andp.201900480 [arXiv:2003.02163 [astro-ph.HE]].

- [4] F. H. Vincent, M. Wielgus, M. A. Abramowicz, E. Gourgoulhon, J. P. Lasota, T. Paumard and G. Perrin, “Geometric modeling of M87* as a Kerr black hole or a non-Kerr compact object,” [arXiv:2002.09226 [gr-qc]].
- [5] V. I. Dokuchaev and N. O. Nazarova, “Modeling the motion of a bright spot in jets from black holes M87* and SgrA*,” [arXiv:2010.01885 [astro-ph.HE]].
- [6] A. Stepanian, S. Khlghatyan and V. G. Gurzadyan, “Black hole shadow to probe modified gravity,” *Eur. Phys. J. Plus* **136** (2021) no.1, 127 doi:10.1140/epjp/s13360-021-01119-2 [arXiv:2101.08261 [gr-qc]].
- [7] N. Cornish, D. Blas and G. Nardini, “Bounding the speed of gravity with gravitational wave observations,” *Phys. Rev. Lett.* **119** (2017) no.16, 161102 doi:10.1103/PhysRevLett.119.161102 [arXiv:1707.06101 [gr-qc]].
- [8] S. W. Hawking, “Particle Creation by Black Holes,” *Commun. Math. Phys.* **43** (1975), 199-220 [erratum: *Commun. Math. Phys.* **46** (1976), 206] doi:10.1007/BF02345020
- [9] S. W. Hawking, “Black Holes and Thermodynamics,” *Phys. Rev. D* **13** (1976), 191-197 doi:10.1103/PhysRevD.13.191
- [10] S. Iyer and C. M. Will, “Black Hole Normal Modes: A {WKB} Approach. 1. Foundations and Application of a Higher Order {WKB} Analysis of Potential Barrier Scattering,” *Phys. Rev. D* **35** (1987), 3621 doi:10.1103/PhysRevD.35.3621
- [11] M. K. Parikh and F. Wilczek, “Hawking radiation as tunneling,” *Phys. Rev. Lett.* **85** (2000), 5042-5045 doi:10.1103/PhysRevLett.85.5042 [arXiv:hep-th/9907001 [hep-th]].
- [12] H. T. Cho and Y. C. Lin, “WKB analysis of the scattering of massive Dirac fields in Schwarzschild black hole spacetimes,” *Class. Quant. Grav.* **22** (2005), 775-790 doi:10.1088/0264-9381/22/5/001 [arXiv:gr-qc/0411090 [gr-qc]].
- [13] R. A. Konoplya and A. Zhidenko, “Passage of radiation through wormholes of arbitrary shape,” *Phys. Rev. D* **81** (2010), 124036 doi:10.1103/PhysRevD.81.124036 [arXiv:1004.1284 [hep-th]].
- [14] S. Dey and S. Chakrabarti, “A note on electromagnetic and gravitational perturbations of the Bardeen de Sitter black hole: quasinormal modes and greybody factors,” *Eur. Phys. J. C* **79** (2019) no.6, 504 doi:10.1140/epjc/s10052-019-7004-0 [arXiv:1807.09065 [gr-qc]].
- [15] R. A. Konoplya and A. F. Zinhailo, “Hawking radiation of non-Schwarzschild black holes in higher derivative gravity: a crucial role of grey-body factors,” *Phys. Rev. D* **99** (2019) no.10, 104060 doi:10.1103/PhysRevD.99.104060 [arXiv:1904.05341 [gr-qc]].
- [16] R. A. Konoplya, A. Zhidenko and A. F. Zinhailo, “Higher order WKB formula for quasinormal modes and grey-body factors: recipes for quick and accurate calculations,” *Class. Quant. Grav.* **36** (2019), 155002 doi:10.1088/1361-6382/ab2e25 [arXiv:1904.10333 [gr-qc]].
- [17] S. Devi, R. Roy and S. Chakrabarti, “Quasinormal modes and greybody factors of the novel four dimensional Gauss–Bonnet black holes in asymptotically de Sitter space time: scalar, electromagnetic and Dirac perturbations,” *Eur. Phys. J. C* **80** (2020) no.8, 760 doi:10.1140/epjc/s10052-020-8311-1 [arXiv:2004.14935 [gr-qc]].
- [18] M. Visser, “Some general bounds for 1-D scattering,” *Phys. Rev. A* **59** (1999), 427-438 doi:10.1103/PhysRevA.59.427 [arXiv:quant-ph/9901030 [quant-ph]].
- [19] P. Boonserm and M. Visser, “Bounding the Bogoliubov coefficients,” *Annals Phys.* **323** (2008), 2779-2798 doi:10.1016/j.aop.2008.02.002 [arXiv:0801.0610 [quant-ph]].
- [20] P. Boonserm, “Rigorous bounds on Transmission, Reflection, and Bogoliubov coefficients,” [arXiv:0907.0045 [math-ph]].
- [21] P. Boonserm, T. Ngampitipan and P. Wongjun, “Greybody factor for black holes in dRGT massive gravity,” *Eur. Phys. J. C* **78** (2018) no.6, 492 doi:10.1140/epjc/s10052-018-5975-x [arXiv:1705.03278 [gr-qc]].
- [22] P. Boonserm, T. Ngampitipan and P. Wongjun, “Greybody factor for black string in dRGT massive gravity,” *Eur. Phys. J. C* **79** (2019) no.4, 330 doi:10.1140/epjc/s10052-019-6827-z [arXiv:1902.05215 [gr-qc]].
- [23] S. Barman, “The Hawking effect and the bounds on greybody factor for higher dimensional Schwarzschild black holes,” *Eur. Phys. J. C* **80** (2020) no.1, 50 doi:10.1140/epjc/s10052-020-7613-7 [arXiv:1907.09228 [gr-qc]].
- [24] A. Chowdhury and N. Banerjee, “Greybody factor and sparsity of Hawking radiation from a charged spherical black hole with scalar hair,” *Phys. Lett. B* **805** (2020), 135417 doi:10.1016/j.physletb.2020.135417 [arXiv:2002.03630 [gr-qc]].
- [25] S. Kanzi, S. H. Mazharimousavi and İ. Sakalli, “Greybody factors of black holes in dRGT massive gravity coupled with nonlinear electrodynamics,” *Annals Phys.* **422** (2020), 168301 doi:10.1016/j.aop.2020.168301 [arXiv:2007.05814 [hep-th]].